THE JOURNAL OF BIOLOGICAL CHEMISTRY VOL. 284, NO. 37, pp. 25116–25125, September 11, 2009

Protein Kinase A Increases Type-2 Inositol 1,4,5-Trisphosphate Receptor Activity by Phosphorylation of Serine 937*[S]

Received for publication, April 17, 2009, and in revised form, June 10, 2009 Published, JBC Papers in Press, July 16, 2009, DOI 10.1074/jbc.M109.010132

Matthew J. Betzenhauser[1], **Jenna L. Fike, Larry E. Wagner II, and David I. Yule**[2]

From the Department of Pharmacology and Physiology, School of Medicine and Dentistry, University of Rochester Medical Center, Rochester, New York 14642

Protein kinase A (PKA) phosphorylation of inositol 1,4,5-trisphosphate receptors ($InsP_3Rs$) represents a mechanism for shaping intracellular Ca^{2+} signals following a concomitant elevation in cAMP. Activation of PKA results in enhanced Ca^{2+} release in cells that express predominantly $InsP_3R2$. PKA is known to phosphorylate $InsP_3R2$, but the molecular determinants of this effect are not known. We have expressed mouse $InsP_3R2$ in DT40-3KO cells that are devoid of endogenous $InsP_3R$ and examined the effects of PKA phosphorylation on this isoform in unambiguous isolation. Activation of PKA increased Ca^{2+} signals and augmented the single channel open probability of $InsP_3R2$. A PKA phosphorylation site unique to the $InsP_3R2$ was identified at Ser^{937}. The enhancing effects of PKA activation on this isoform required the phosphorylation of Ser^{937}, since replacing this residue with alanine eliminated the positive effects of PKA activation. These results provide a mechanism responsible for the enhanced Ca^{2+} signaling following PKA activation in cells that express predominantly $InsP_3R2$.

Hormones, neurotransmitters, and growth factors stimulate the production of $InsP_3$[3] and Ca^{2+} signals in virtually all cell types (1). The ubiquitous nature of this mode of signaling dictates that this pathway does not exist in isolation; indeed, a multitude of additional signaling pathways can be activated simultaneously. A prime example of this type of "cross-talk" between independently activated signaling systems results from the parallel activation of cAMP and Ca^{2+} signaling pathways (2, 3). Interactions between these two systems occur in numerous distinct cell types with various physiological consequences (3–6). Given the central role of $InsP_3R$ in Ca^{2+} signaling, a major route of modulating the spatial and temporal features of Ca^{2+} signals following cAMP production is potentially through PKA phosphorylation of the $InsP_3R$ isoform(s) expressed in a particular cell type.

There are three $InsP_3R$ isoforms ($InsP_3R1$, $InsP_3R2$, and $InsP_3R3$) expressed to varying degrees in mammalian cells (7, 8). $InsP_3R1$ is the major isoform expressed in the nervous system, but it is less abundant compared with other subtypes in non-neuronal tissues (8). Ca^{2+} release via $InsP_3R2$ and $InsP_3R3$ predominate in these tissues. $InsP_3R2$ is the major $InsP_3R$ isoform in many cell types, including hepatocytes (7, 8), astrocytes (9, 10), cardiac myocytes (11), and exocrine acinar cells (8, 12). Activation of PKA has been demonstrated to enhance $InsP_3$-induced Ca^{2+} signaling in hepatocytes (13) and parotid acinar cells (4, 14). Although PKA phosphorylation of $InsP_3R2$ is a likely causal mechanism underlying these effects, the functional effects of phosphorylation have not been determined in cells unambiguously expressing $InsP_3R2$ in isolation. Furthermore, the molecular determinants of PKA phosphorylation of this isoform are not known.

PKA-mediated phosphorylation is an efficient means of transiently and reversibly regulating the activity of the $InsP_3R$. $InsP_3R1$ was identified as a major substrate of PKA in the brain prior to its identification as the $InsP_3R$ (15, 16). However, until recently, the functional consequences of phosphorylation were unresolved. Initial conflicting results were reported indicating that phosphoregulation of $InsP_3R1$ could result in either inhibition or stimulation of receptor activity (16, 17). Mutagenic strategies were employed by our laboratory to clarify this discrepancy. These studies unequivocally assigned phosphorylation-dependent enhanced Ca^{2+} release and $InsP_3R1$ activity at the single channel level, through phosphorylation at canonical PKA consensus motifs at Ser^{1589} and Ser^{1755}. The sites responsible were also shown to be specific to the particular $InsP_3R1$ splice variant (18). These data were also corroborated by replacing the relevant serines with glutamates in a strategy designed to construct "phosphomimetic" $InsP_3R1$ by mimicking the negative charge added by phosphorylation (19, 20). Of particular note, however, although all three isoforms are substrates for PKA, neither of the sites phosphorylated by PKA in $InsP_3R1$ are conserved in the other two isoforms (21). Recently, three distinct PKA phosphorylation sites were identified in $InsP_3R3$ that were in different regions of the protein when compared with $InsP_3R1$ (22). To date, no PKA phosphorylation sites have been identified in $InsP_3R2$.

Interactions between Ca^{2+} and cAMP signaling pathways are evident in exocrine acinar cells of the parotid salivary gland. In these cells, both signals are important mediators of fluid and protein secretion (23). Multiple components of the $[Ca^{2+}]_i$

* This work was supported, in whole or in part, by National Institutes of Health Grants RO1-DK054568 and RO1-DE016999 (to D. I. Y.).

[S] The on-line version of this article (available at http://www.jbc.org) contains supplemental Fig. S1.

[1] Supported by NIDCR, National Institutes of Health, Training Grant T32-DE07202.

[2] To whom correspondence should be addressed: 601 Elmwood Ave., Box 711, Rochester, NY 14642. Tel.: 585-273-2154; Fax: 585-273-2652; E-mail: David_Yule@urmc.rochester.edu.

[3] The abbreviations used are: $InsP_3$, inositol 1,4,5-trisphosphate; $InsP_3R$, $InsP_3$ receptor; CCh, carbachol; M3R, human muscarinic M3R; PKA, protein kinase A; cBIMPs, 5,6-dichloro-1-β-D-ribofuranosylbenzylimadazole-3′,5′-cyclic monophosphorothioate; GFP, green fluorescent protein; EGFP, enhanced GFP; IBMX, isobutylmethylxanthine; BAPTA, 1,2-bis(2-aminophenoxy)ethane-*N*,*N*,*N*′,*N*′-tetraacetic acid.

signaling pathway in these cells are potential substrates for modulation by PKA. Previous work from this laboratory established that activation of PKA potentiates muscarinic acetylcholine receptor-induced $[Ca^{2+}]_i$ signaling in mouse and human parotid acinar cells (4, 24, 25). A likely mechanism to explain this effect is that PKA phosphorylation increases the activity of $InsP_3R$ expressed in these cells. Consistent with this idea, activation of PKA enhanced $InsP_3$-induced Ca^{2+} release in permeabilized mouse parotid acinar cells and also resulted in the phosphorylation of $InsP_3R2$ (4).

Invariably, prior work examining the functional effects of PKA phosphorylation on $InsP_3R2$ has been performed using cell types expressing multiple $InsP_3R$ isoforms. For example, AR4-2J cells are the preferred cell type for examining $InsP_3R2$ in relative isolation, because this isoform constitutes more than 85% of the total $InsP_3R$ population (8). $InsP_3R1$, however, contributes up to ~12% of the total $InsP_3R$ in AR4-2J cells. An initial report using $InsP_3$-mediated $^{45}Ca^{2+}$ flux suggested that PKA activation increased $InsP_3R$ activity in AR4-2J cells (21). A similar conclusion was made in a later study, which documented the effects of PKA activation on agonist stimulated Ca^{2+} signals in AR4-2J cells (26). Any effects of phosphorylation observed in these experiments could plausibly have resulted from phosphorylation of the residual $InsP_3R1$.

Although PKA enhances $InsP_3$-induced calcium release in cells expressing predominantly $InsP_3R2$, including hepatocytes, parotid acinar cells, and AR4-2J cells (4, 13, 21, 26, 27), $InsP_3R2$ is not phosphorylated at stoichiometric levels by PKA (21). This observation has called into question the physiological significance of PKA phosphorylation of $InsP_3R2$ (28). The apparent low levels of $InsP_3R2$ phosphorylation are clearly at odds with the augmented Ca^{2+} release observed in cells expressing predominantly this isoform. The equivocal nature of these findings probably stems from the fact that, to date, all of the studies demonstrating positive effects of PKA activation on Ca^{2+} release were conducted in cells that also express $InsP_3R1$. The purpose of the current experiments was to analyze the functional effects of phosphorylation on $InsP_3R2$ expressed in isolation on a null background. We report that $InsP_3R2$ activity is increased by PKA phosphorylation under these conditions, and furthermore, we have identified a unique phosphorylation site in $InsP_3R2$ at Ser^{937}. In total, these results provide a direct mechanism for the cAMP-induced activation of $InsP_3R2$ via PKA phosphorylation of $InsP_3R2$.

EXPERIMENTAL PROCEDURES

cDNA Expression Constructs—Mouse $InsP_3R2$ cDNA, a kind gift of Dr. Katsuhiko Mikoshiba (Riken, Japan), was used as the template for creation of EGFP-tagged subclones (29). All fragments were amplified by PCR with MluI and NotI restriction sites incorporated into the N termini and C termini, respectively. A BssHII site was incorporated into the N terminus of fragment 3 because of an internal MluI site in this fragment. PCR products were ligated with MluI- and NotI-digested pCI-Neo-EGFP (a kind gift from Dr. Sundeep Malik, University of Rochester) to create the mammalian expression vectors. The full-length rat $InsP_3R2$ in the expression vector pCMV5 was a kind gift of Dr. Suresh Joseph (Thomas Jefferson University). A Kozak initiation motif was engineered into the receptor DNA using PCR. The modified receptor DNA was then cloned into the pEF6/V5-His Topo TA expression vector (Invitrogen).

Mutagenesis—All point mutations in the $InsP_3R2$ fragments were created using QuikChange XL or QuikChange multisite mutagenesis (Stratagene, La Jolla, CA). Point mutations in the full-length $InsP_3R2$ expression constructs to allow S937A and S2633A amino acid substitutions were constructed using a two-step QuikChange mutagenesis strategy (30).

DT40 Cell Lines—The cDNA construct for 3× hemagglutinin-tagged human type-3 muscarinic receptor (M3R) and wild type and mutated $InsP_3R2$ constructs were linearized with MfeI. Linearized constructs were introduced into DT40-3KO cells, which are devoid of $InsP_3R$, by nucleofection using an Amaxa nucleofector as described previously (31–33). After nucleofection, the cells were incubated in growth medium for 24 h prior to dilution in selection medium containing 2 mg/ml Geneticin. Cells were then seeded into 96-well tissue culture plates at ~1000 cells/well and incubated in selection medium for at least 7 days. Wells exhibiting growth after the selection period were picked for expansion.

Phosphorylation of $InsP_3R2$ in Intact Cells—COS-7 cells were transfected with $InsP_3R2$ expression constructs 36–40 h prior to labeling with $^{32}PO_4^-$ for 2 h in phosphate-free Dulbecco's modified Eagle's medium. ~150 μCi were added to 1 ml of phosphate-free media in each well of a 6-well culture dish. After labeling, cells were washed three times in Tris-buffered saline, treated with forskolin for 15 min, and lysed in lysis buffer (10 mM Tris, 150 mM NaCl, 100 mM NaF, 1 EDTA, 1% Nonidet P-40, pH 7.4) supplemented with protease inhibitor tablets (Roche Applied Science). Lysates were cleared with pansorbin prior to incubation with immunoprecipitation antibody for 2 h. Protein A/G beads were then added for 1 h. The beads were washed three times in lysis buffer and resuspended in Laemmli sample buffer. Samples were separated by PAGE on 5% polyacrylamide, and the gels were dried for phosphorimaging using a phosphor storage screen (Amersham Biosciences) and Amersham Biosciences PhosphorImager.

PKA Phosphorylation of $InsP_3R$ in Vitro—COS-7 cells were transfected with wild type or mutated $InsP_3R2$ expression constructs 36–40 h before harvest. Cells were washed twice in phosphate-buffered saline prior to suspension in lysis buffer supplemented with protease inhibitor mixture tablets (Roche Applied Science). Cells were dispersed using a cell scraper (Corning Glass) and allowed to incubate on ice for 20 min. Lysates were cleared with pansorbin prior to incubation with immunoprecipitation antibody for 2 h. Protein A/G beads were then added for 1 h. The beads were washed three times in lysis buffer and three times in PKA phosphorylation buffer (120 mM KCl, 50 mM Tris, 0.1% Triton X-100, 0.3 mM $MgCl_2$, pH 7.2) and resuspended in phosphorylation buffer.

20 units of purified recombinant PKA (Promega) were added to the samples along with [γ-^{32}P]ATP (~5 μCi/reaction) and 0.5 μM unlabeled ATP. Kinase reactions were incubated for 0–15 min, and the beads were washed six times in lysis buffer prior to resuspension and SDS-PAGE. Gels were stained with BioSafe Coomassie (Bio-Rad) and subsequently dried down for

phosphorimaging. ^{32}P signals were detected by phosphorimaging as described above.

Antibodies—Rabbit polyclonal antibodies designed against a specific sequence in the rat $InsP_3R2$ extreme C terminus (α-$InsP_3R2$-CT; ^{2686}GFLGSNTPHENHHMPPH^{2702}) were generated by Pocono Rabbit Farms & Laboratories (Canadensis, PA). A rabbit polyclonal antibody against the region surrounding phosphorylated Ser^{937} of mouse $InsP_3R2$ (^{934}SRGpSIFPVSVPDAC^{946}, where pS represents phosphoserine) was generated by Quality Controlled Biochemicals (Hopkinton, MA).

Phosphorylation of $InsP_3R2$ Serine 937 in COS-7 Cells and Mouse Parotid Acinar Cells—Mouse parotid acinar cells were isolated by collagenase digestion, as described previously (4). COS-7 cells or mouse parotid acinar cells were treated with 10 μM forskolin and 100 μM IBMX for 15 min. Cell lysates were harvested in lysis buffer supplemented with 100 nM okadaic acid. $InsP_3R2$ was immunoprecipitated from cell lysates using α-$InsP_3R2$-CT. Where noted, some immunoprecipitated samples were treated with 10 units of calf intestinal alkaline phosphatase (New England Biolabs, Ipswich, MA) at 37 °C for 1 h. Samples were separated on SDS-PAGE, and phosphorylated serine 937 was detected with α-$Ser(P)^{937}$ by Western blotting. Blots were stripped and reprobed with α-$InsP_3R2$-CT to verify equal amounts of total immunoprecipitated $InsP_3R2$.

Digital Imaging of Intracellular Ca^{2+} in DT40 Cells—DT40 cells were loaded with 2 μM of the Ca^{2+}-sensitive dye Fura-2 AM at room temperature for 15–30 min. Fura-2-loaded cells were allowed to adhere to a glass coverslip at the bottom of a perfusion chamber. Cells were perfused in HEPES-buffered physiological saline containing 137 mM NaCl, 0.56 mM $MgCl_2$, 4.7 mM KCl, 1 mM Na_2HPO_4, 10 mM HEPES, 5.5 mM glucose, and 1.26 mM $CaCl_2$, pH 7.4. Imaging was performed using an inverted Nikon microscope through a ×40 oil immersion objective lens (numerical aperture, 1.3). Fura-2-loaded cells were excited alternately with light at 340 and 380 nm by using a monochrometer-based illumination system (TILL Photonics), and the emission at 510 nm was captured by using a digital frame transfer CCD camera. In experiments where $InsP_3R$ or M3R were transiently expressed, cDNA encoding HcRed was included to indicate transfected cells. HcRed fluorescence was detected by excitation at 560 nm and observing the emission at >600 nm.

Single Channel Recordings—Whole cell patch clamp recordings of single $InsP_3R2$ channel activity present in the plasma membrane (34, 35) were made from DT40-3KO cells stably expressing mouse $InsP_3R2$. K^+ was utilized as the charge carrier in all experiments, and free Ca^{2+} was clamped at 200 nM to favor activation of $InsP_3R$ (bath: 140 mM KCl, 10 mM HEPES, 500 μM BAPTA, free Ca^{2+} 250 nM (pH 7.1); pipette: 140 mM KCl, 10 mM HEPES, 100 μM BAPTA, 200 nM free Ca^{2+}, 5 mM Na_2-ATP unless otherwise noted (pH 7.1)). Borosilicate glass pipettes were pulled and fire-polished to resistances of about 20 megaohms. Following establishment of stable high resistance seals, the membrane patches were ruptured to form the whole cell configuration with resistances >5 gigaohms and capacitances of >8 picofarads. Currents were recorded under voltage clamp conditions at −100 mV using an Axopatch 200B amplifier and pClamp 9. Channel recordings were digitized at 20 kHz and filtered at 5 kHz with a −3 dB, 4-pole Bessel filter. Activity was typically evident essentially immediately following breakthrough with $InsP_3$ in the pipette. Analyses were performed using the event detection protocol in Clampfit 9. Channel openings were detected by half-threshold crossing criteria. We assumed that the number of channels in any particular cell is represented by the maximum number of discrete stacked events observed during the experiment. The single channel open probability (P_o) was calculated using the multimodal distribution for the open and closed current levels.

RESULTS

Activation of PKA Enhances Ca^{2+} Signaling in DT40-M3 Cells Expressing Mouse $InsP_3R2$—Analyzing subtype-specific regulation of individual $InsP_3R$ isoforms in native tissue is hampered by the fact that most mammalian cell types express multiple isoforms and that the functional receptors can form heterotetrameric channels (36–38). Given these limitations, the functional properties of specific homotetrameric receptors must be determined in a defined system. Kurosaki and colleagues (40) developed such a system based on the DT40 chicken B-cell precursor line by creating a null background (DT40-3KO cells) following elimination of all three $InsP_3R$ isoforms through homologous recombination (39, 40). In order to examine the effects of PKA phosphorylation on InsP3R2, we transiently expressed this isoform in a DT40-3KO cell line (DT40-M3) stably expressing the human M3R (33).

DT40-M3 cells transfected with mouse $InsP_3R2$ cDNA, identified by expression of HcRed, responded to the muscarinic agonist carbachol (CCh) stimulation in a concentration-dependent manner (Fig. 1*A*). Treatment with 1 μM CCh produced Ca^{2+} signals with a range of amplitudes, presumably as a consequence of a range of $InsP_3R2$ expression levels following transient transfection (Fig. 1*B*). Cells that responded to 1 μM CCh with amplitudes no greater than 0.2 340 nm/380 nm ratio units were used for the purposes of analyzing the effects of raising cAMP. An example of a DT40-M3 cell expressing mouse $InsP_3R2$ and treated three times with 1 μM CCh is shown in Fig. 1*C*. Treatment of cells with 20 μM forskolin after the first CCh treatment resulted in Ca^{2+} transients with >5-fold larger amplitudes as shown in Fig. 1*C*, indicating that activation of PKA enhances Ca^{2+} release from $InsP_3R2$. This effect was only evident in cells that responded submaximally to 1 μM CCh. As previously observed, forskolin induced a rise in $[Ca^{2+}]_i$ in some cells (27). This effect was evident in ~50% of cells from six separate experiments, and these cells were excluded from analysis. The mechanism underlying this effect is presently unknown; however, it is independent of $InsP_3R$ as it occurs in DT40-3KO cells at approximately the same frequency. The activation of PKA by this treatment had clear enhancing effects on the Ca^{2+} signal (Fig. 1*D*).

We also obtained additional evidence that PKA-induced phosphorylation results in increased $InsP_3R2$ activity by examining the effects of activating PKA on the single channel activity of $InsP_3R2$. Single $InsP_3R2$ measurements were conducted using whole cell recordings of plasma membrane-resident $InsP_3R2$ in DT40 cells stably expressing $InsP_3R2$ (20, 31, 34, 35,

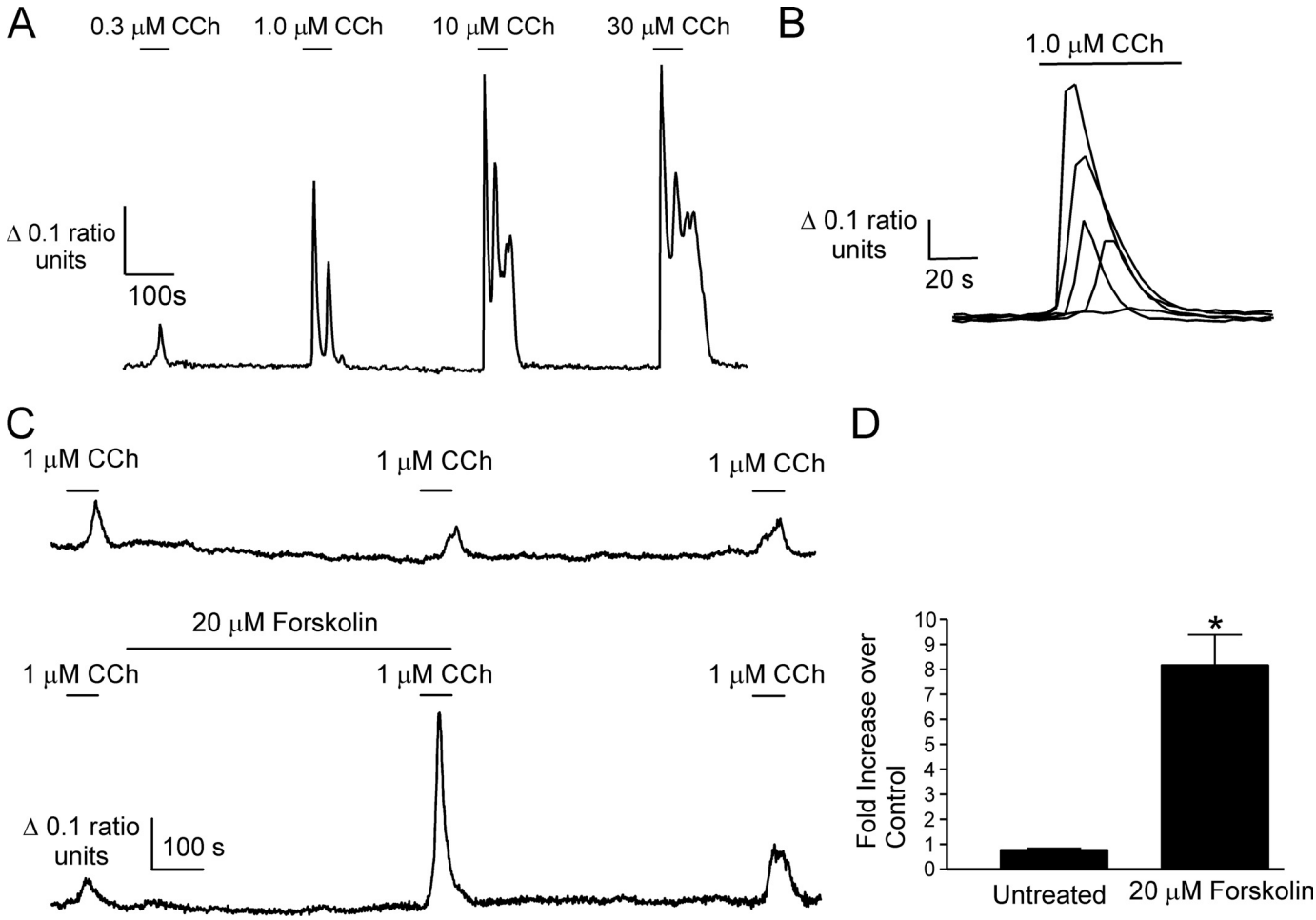

FIGURE 1. **Forskolin enhances CCh-evoked Ca^{2+} responses in DT40-M3 cells expressing mouse $InsP_3R2$.** An expression construct harboring cDNA for mouse $InsP_3R2$ was introduced into DT40-M3 cells. *A*, a representative Fura-2 recording from a single cell showing increasing Ca^{2+}-transient amplitudes with increasing CCh concentrations. *B*, the range of Ca^{2+} signal amplitudes observed in five cells from a single experiment to stimulation with 1 μM CCh. *C*, *upper trace*, a Fura-2 recording from a DT40-M3 cell expressing mouse $InsP_3R2$ stimulated three times with 1 μM CCh ($n = 3$ experimental runs). *Lower trace*, the effect of raising cAMP with forskolin on a 1 μM CCh-evoked Ca^{2+} transient ($n = 5$ experimental runs). *D*, pooled data from the indicated number of experiments comparing the second 1 μM CCh treatment with the first in the absence and presence of forskolin (*, $p \leq 0.05$, Student's unpaired *t* test).

41). This configuration allows the monitoring of single $InsP_3R$ channels during the activation of endogenous PKA following exposure to forskolin (20). Fig. 2*A* shows an example of channel activity when low concentrations of $InsP_3$ (100 nM) were included in the recording pipette. No channel activity is observed in this preparation in the absence of $InsP_3$ or in DT40-3KO cells devoid of $InsP_3R$ (31). The open probability of the channel was markedly enhanced following exposure to forskolin (Fig. 2, *B* (diary plot for representative cell) and *C* (pooled data)). $InsP_3R2$ channel activity returned to pre-PKA activation levels following washout of forskolin. Enhanced channel activity was readily evident at threshold [$InsP_3$] but not observed at higher levels of $InsP_3$ (1 μM; Fig. 2*C*). In total, these data provide clear evidence that activation of PKA results in enhanced Ca^{2+} release through increased activity of $InsP_3R2$.

PKA Phosphorylates Mouse $InsP_3R2$ at Serine 937—A likely mechanism for the positive effects of increasing cAMP on the Ca^{2+} signal is through direct phosphorylation of $InsP_3R2$ by PKA. Because this signaling system is a rich source of potential PKA substrates, we cannot, however, discount other effects of PKA on the M3R-induced Ca^{2+} signals. Potential loci might include effects on $InsP_3$ levels, Ca^{2+} clearance, or Ca^{2+} entry. In addition, cAMP at millimolar concentrations was recently reported to enhance Ca^{2+} release from $InsP_3R2$ by a mechanism that did not require PKA activity (42). Establishing the PKA phosphorylation site(s) and subsequently performing mutagenesis of the putative sites in $InsP_3R2$ are required to definitively rule out these and other possible mechanisms for the increased Ca^{2+} signal. Although PKA has been shown to phosphorylate $InsP_3R2$ in a number of studies by independent groups (21, 26, 28), the site(s) of phosphorylation are not known. Experiments were performed following transient overexpression of $InsP_3R2$ in COS-7 cells. This expression system was chosen because of low endogenous levels of $InsP_3R$ and the high transfection efficiency such that expressed receptor can be readily distinguished from endogenous protein (see supplemental Fig. S1). In addition, expressed receptors rarely form heterotetramers with endogenous $InsP_3R$ (43). Fig. 3 and the supplemental material confirm that $InsP_3R2$ is a substrate for PKA. Both mouse and rat $InsP_3R2$ were phosphorylated in intact cells (Fig. 3*A* and supplemental Fig. S1) and *in vitro* (Fig. 3*B*). Fig. 3*C* shows alignments of mammalian $InsP_3R$ protein

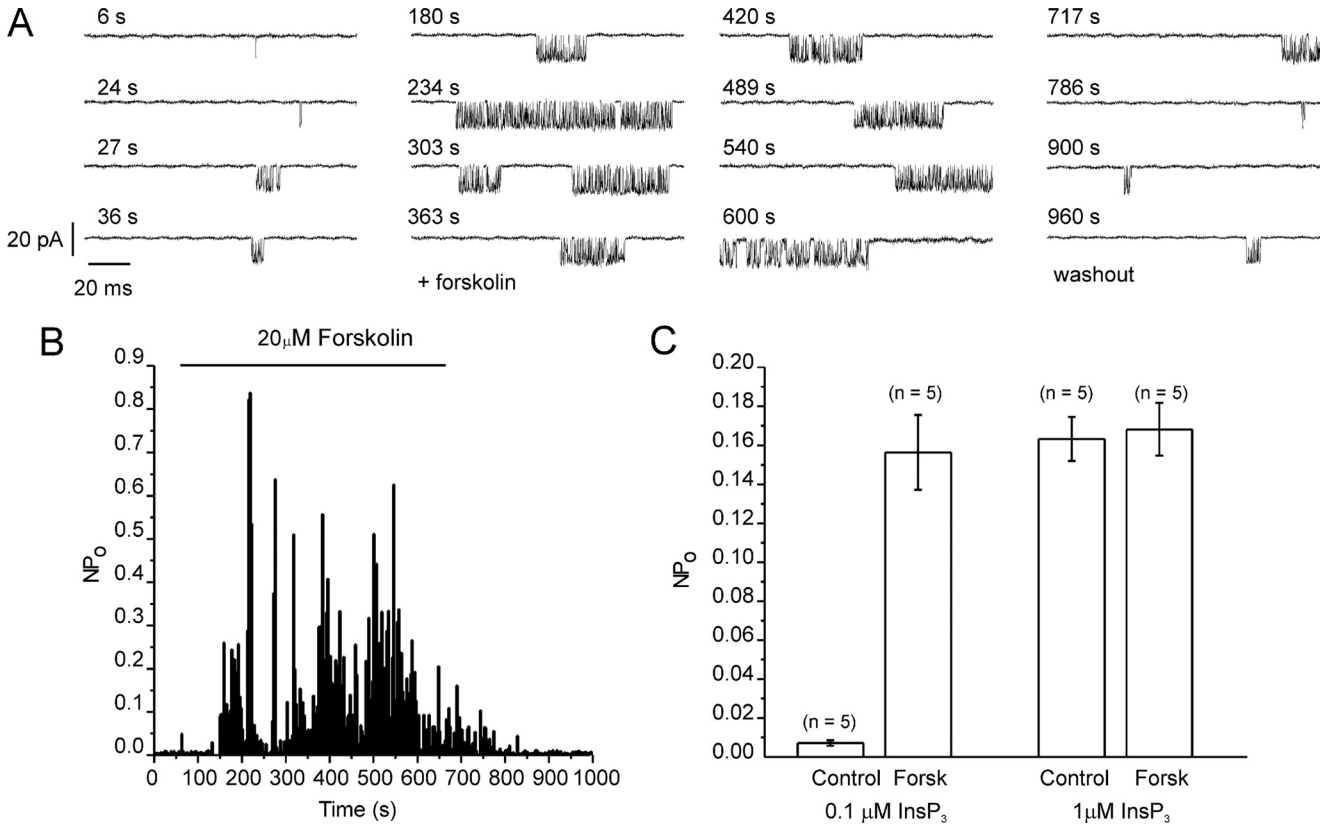

FIGURE 2. **Activation of PKA results in increased $InsP_3R2$ single channel activity.** Whole cell patch clamp recordings were made in DT40-3KO cells stably expressing $InsP_3R2$. *A*, representative sweeps from cells at a holding potential of −100 mV. Channel activity is observed with 100 nM $InsP_3$ in the patch pipette. The activity is markedly enhanced following exposure to forskolin, which was applied at 60 s and removed at 660 s, as indicated by the *bar* in *B*. *B*, a diary plot of activity during each sweep. *C*, pooled data from experiments with both 100 nM and 1 μM $InsP_3$.

sequences around the known phosphorylation sites in $InsP_3R1$ and $InsP_3R3$. None of these sites are conserved in $InsP_3R2$ sequences, indicating that the phosphorylation evident in Fig. 3, *A* and *B*, occurs at a novel PKA phosphorylation site(s).

Optimal PKA phosphorylation sites are serines or threonines preceded by basic residues at the −2- and −3-positions (44). The primary amino acid sequences of individual mammalian $InsP_3R2$ proteins combined harbor greater than 300 serine and threonine residues. Of these potential candidates, ~30 have basic residues (arginine or lysine) upstream of the putative target serine or threonine. The single canonical PKA consensus sequence located in $InsP_3R2$ ($RRPS^{2508}$) is probably not accessible to the kinase, because it is located on the luminal side of the putative permeability (P) loop. Given the large number of potential putative PKA phosphorylation sites present in the primary sequence of $InsP_3R2$, we developed a subcloning approach to identify novel PKA phosphorylation sites.

Limited trypsin digestion of $InsP_3R1$ and $InsP_3R3$ has established that $InsP_3R$ can be divided into five (in the case of $InsP_3R1$) or four (in the case of $InsP_3R3$) globular domains with intervening solvent-exposed trypsin digestion sites (22, 45, 46). In order to maintain domain structure as much as possible, $InsP_3R2$ subclones were designed to correspond with predicted limited trypsin digestion products. The $InsP_3R2$ sequence was therefore divided into five smaller fragment constructs with EGFP as an epitope tag on the N terminus of each fragment. As depicted in Fig. 4*A*, fragment 1 corresponded with residues 1–343, fragment 2 with residues 344–919, fragment 3 with residues 920–1583, fragment 4 with residues 1584–1883, and fragment 5 with residues 1884–2701.

Constructs coding for the five fragments were transfected into COS-7 cells and immunoprecipitated with an antibody directed against EGFP. A separate sample was transfected with a construct coding for enhanced yellow fluorescent protein-tagged $InsP_3R1$ and served as a positive control. Immunoprecipitated proteins were subjected to *in vitro* PKA kinase assays, as described under "Experimental Procedures." Samples were then resolved by SDS-PAGE, and ^{32}P incorporation was determined by phosphorimaging. ^{32}P was incorporated into the enhanced yellow fluorescent protein-$InsP_3R1$ samples as well as into samples from cells expressing fragment 3 and fragment 5 (Fig. 4*B*). Fig. 4*C* shows a Western blot probed with α-GFP antibody of the various fragments. Fragment 4, which contains a putative PKA phosphorylation site ($KKDS^{1687}$) did not incorporate ^{32}P under these conditions (Fig. 4*B*). Because fragment 4 was somewhat weakly expressed compared with the other fragments, these data do not formally rule out the possibility that a functional PKA-phosphorylation site is present in this domain (but see subsequent functional data). Nevertheless, these results indicate that PKA phosphorylation sites in $InsP_3R2$ are probably harbored between residues 920 and 1583 and between residues 1884 and 2701 (Fig. 4*A*).

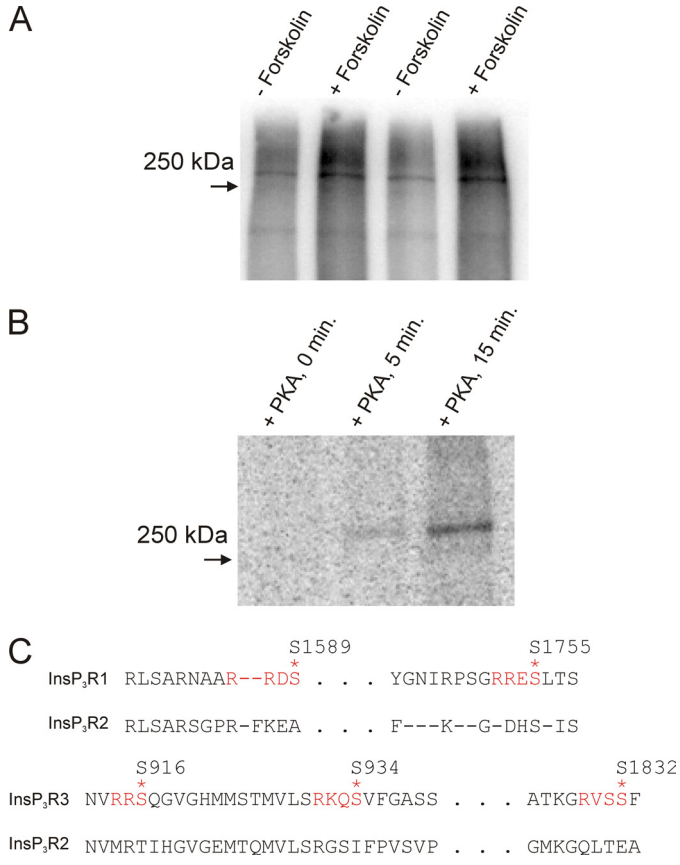

FIGURE 3. **Mammalian InsP$_3$R2 is phosphorylated in response to raising cAMP in metabolically labeled COS-7 cells and *in vitro* by purified PKA.** COS-7 cells were transfected with mouse InsP$_3$R2 cDNA (*A*). 36 h after transfection, cells were metabolically labeled with $^{32}PO_4^-$ prior to forskolin treatment, immunoprecipitation, and PAGE. *A*, phosphor image of a dried gel loaded with samples from mouse InsP$_3$R2-expressing cells. Greater ^{32}P incorporation into a ~250 kDa band in the forskolin-treated transfected samples indicated phosphorylation of InsP$_3$R2. *B*, mouse InsP$_3$R2 was immunoprecipitated from COS-7 cells and incubated with purified PKA at 37 °C in the presence of [γ-^{32}P]ATP for the indicated times. Results are representative of at least two separate experiments for each condition. *C*, alignments of InsP$_3$R sequences around the PKA phosphorylation sites in InsP$_3$R1 and InsP$_3$R3. None of the sites present in these isoforms are present in InsP$_3$R2.

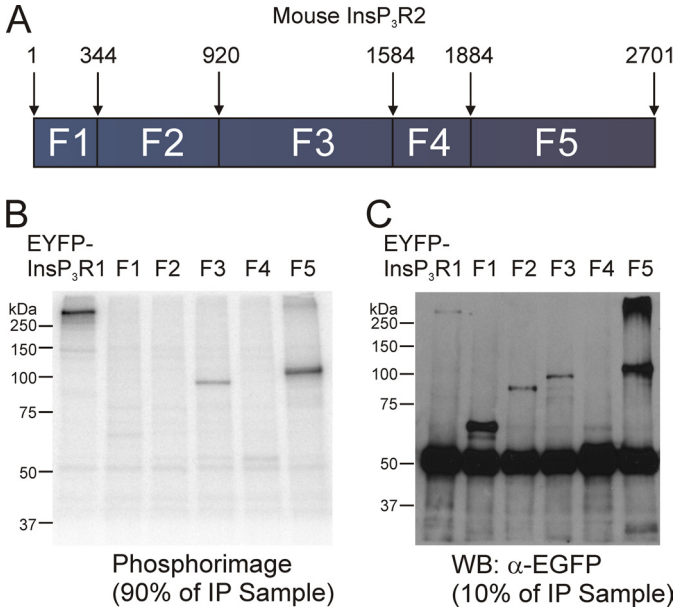

FIGURE 4. **PKA phosphorylates two different fragments of mouse InsP$_3$R2.** *A*, a schematic diagram depicting the boundaries of the fragments used to identify PKA-phosphorylated residues in mouse InsP$_3$R2. The predicted sizes of the EGFP-tagged subclones are as follows: EGFP-F1, ~65 kDa; EGFP-F2, ~94 kDa; EGFP-F3, ~102 kDa; EGFP-F4, ~60 kDa; EGFP-F5, ~120 kDa. EGFP-tagged subclones of mouse InsP$_3$R2 were expressed in COS-7 cells, immunoprecipitated, and then subjected to *in vitro* PKA assays prior to PAGE. *B*, phosphor image from 90% of the immunoprecipitated sample. ^{32}P was incorporated into samples containing enhanced yellow fluorescent protein-InsP$_3$R1, EGFP-fragment 3, and EGFP-fragment 5. *C*, a Western blot with the remaining 10% of the immunoprecipitated samples from *B* probed with α-GFP. Bands of the appropriate sizes indicate the successful immunoprecipitation of all five fragments.

There are 5 serine residues present on fragment 3. Each of these serines was mutated to an alanine in isolation. Mutated fragment 3 was also generated with all 5 serines replaced with alanines. Immunoprecipitated wild type and mutated fragment 3 fusion proteins were subjected to *in vitro* PKA kinase reactions. The serine-free fragment 3 protein did not incorporate ^{32}P (Fig. 5*A*). PKA phosphorylation was also completely eliminated by mutation of Ser^{937} alone (Fig. 5*A*). An arginine precedes Ser^{937} at position 935, fulfilling the minimum requirement for a PKA phosphorylation site. Ser^{937} is unique to InsP$_3$R2, and it is present in all InsP$_3$R2 sequences in the NCBI databases, thus making it a promising candidate serine for physiological PKA phosphorylation. Furthermore, the corresponding region in InsP$_3$R3 contains two of the three PKA phosphorylation sites (Ser^{916} and Ser^{934}), making fragment 3 a likely common region for modulation. Two candidate PKA phosphorylation sites present in the sequence for InsP$_3$R2-fragment 5 corresponding to Ser^{2508} and Ser^{2633} in the full-length sequence were also mutated. Fig. 5*B* shows the results from *in vitro* PKA reactions with these mutations along with a fragment 5 fusion truncated at position 2512. Kinase reactions with the truncation mutant or the S2633A mutant failed to result in ^{32}P incorporation, whereas phosphorylation was unaffected by the S2508A mutation, indicating that the PKA phosphorylation site on fragment 5 occurs exclusively at Ser^{2633}.

Serine 2633 is located in a consensus Akt phosphorylation site (RMRAMS^{2633}), and this putative Akt phosphorylation site is present in all three InsP$_3$R isoforms. Ser^{2633} has also been identified as a *bona fide* Akt phosphorylation site in InsP$_3$R1 by two groups (47, 48). This site is, however, unlikely to represent a PKA site in the context of the full-length InsP$_3$R2, since mutation of the known PKA phosphorylation sites in InsP$_3$R1 and InsP$_3$R3 completely eliminated PKA-induced ^{32}P incorporation *in vitro* and in intact cells (22, 49). Presumably, expression of the truncated receptor renders Ser^{2633} more accessible to PKA. This could result from an altered conformation of the truncated protein. Regardless of whether Ser^{2633} is a substrate of PKA in the full-length receptor, Ca^{2+} release was still increased in cells expressing S2633A mutated InsP$_3$R2 following PKA activation in DT40-M3 cells (Fig. 5*D*).

The sequence surrounding Ser^{937} shows considerable divergence from InsP$_3$R1 and InsP$_3$R3, making the region attractive for the design of a phospho-specific antibody. Similar strategies have been used to produce antibodies recognizing phosphorylated residues in InsP$_3$R1 and InsP$_3$R3 (22, 50). We designed an antibody to specifically recognize phosphorylated Ser^{937} in InsP$_3$R2 (α-Ser(P)^{937}). This antibody failed to recognize InsP$_3$R2 immunoprecipitated from untreated COS-7 cells;

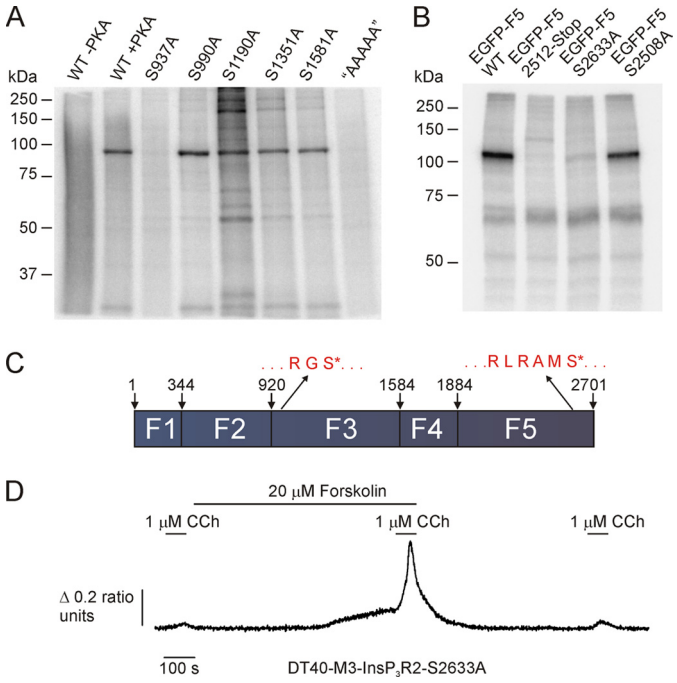

FIGURE 5. **PKA phosphorylates fragment 3 of mouse $InsP_3R2$ at Ser^{937} and fragment 5 at Ser^{2633}.** Mutants in $InsP_3R2$ fragment 3 were generated corresponding to Ser^{937}, Ser^{990}, Ser^{1190}, Ser^{1351}, and Ser^{1581}. Another mutant harboring all five mutations was also generated (*AAAAA*). *A*, the phosphor image from an *in vitro* PKA assay with wild type, S937A, S990A, S1190A, S1351A, S1581A, and "AAAAA" mutated fragment 3 fusions. PKA phosphorylated all fragments except S937A and "AAAAA," indicating that Ser^{937} is the sole PKA phosphorylation site in fragment 3 of mouse $InsP_3R2$. Mutations in fragment 5 corresponding to S2508A, a truncation at 2512, and S2633A were generated. *B*, phosphor image from an *in vitro* PKA assay with these samples. PKA phosphorylated the wild type and S2508A mutated fragment 5 fusions but failed to phosphorylate the truncated or S2633A mutated fusions. *C*, schematic diagram depicting the positions of the Ser^{937} and Ser^{2633} phosphorylation sites in the context of the full-length mouse $InsP_3R2$. *D* shows that, following PKA activation, Ca^{2+} signals are still augmented in cells expressing $InsP_3R2$ S2633A.

however, the antibody readily reported a band in samples immunoprecipitated from forskolin-treated cells (Fig. 6*A*). Importantly, no signal was detected in parallel samples that were treated with alkaline phosphatase following immunoprecipitation. These data indicate that antibody recognition requires the presence of a phosphate group. Similarly, no signal was detected in samples immunoprecipitated from forskolin/IBMX-treated cells expressing S937A mutated $InsP_3R2$. These results clearly show that mouse $InsP_3R2$ can be phosphorylated at Ser^{937} by endogenous PKA, further enforcing the idea that $InsP_3R2$ is a physiological substrate of PKA.

These data demonstrating that PKA phosphorylates $InsP_3R2$ at Ser^{937} were obtained using overexpressed recombinant $InsP_3R2$. In order to determine if PKA can phosphorylate endogenous $InsP_3R2$, we also probed for phosphorylation of Ser^{937} in $InsP_3R2$ immunoprecipitated from mouse parotid acinar cells. We have demonstrated previously that forskolin treatment induces the apparent phosphorylation of $InsP_3R2$ (4). In these experiments, $InsP_3R2$ was detected in samples immunoprecipitated from forskolin-treated cells with an anti-phospho-Ser/Thr antibody. This experimental paradigm could not formally rule out the possibility that the apparent detection of phosphorylated $InsP_3R2$ was the result of co-immunoprecipitation of non-phosphorylated $InsP_3R2$ originally present in a heterotetrameric complex with phosphorylated $InsP_3R1$. As shown in Fig. 6*B*, the α-$Ser(P)^{937}$ antibody clearly recognized phosphorylated $InsP_3R2$ in samples that were immunoprecipitated from forskolin/IBMX-treated parotid acinar cells but not in untreated cells. These results provide strong evidence that PKA phosphorylates endogenously expressed $InsP_3R2$ at Ser^{937}.

Replacement of Serine 937 with Alanine Eliminates the Enhancing Effects of PKA on $InsP_3R2$—The results described above clearly demonstrate that PKA phosphorylates $InsP_3R2$ at Ser^{937}. We next sought to determine if this site is responsible for the positive effects of raising cAMP illustrated in Fig. 1. We generated a stable cell line expressing $InsP_3R2$-S937A and compared the effects of PKA activation on Ca^{2+} signals with those of a cell line stably expressing wild type $InsP_3R2$ (31). The cell lines were transiently transfected with the M3R to allow repeated stimulations with CCh. In these experiments, we utilized 5,6-dichloro-1-β-D- ribofuranosylbenzylimadazole-3′,5′-cyclic monophosphorothioate (cBIMPs), a specific, highly cell-permeable cAMP analogue, to activate PKA. Unlike forskolin, this treatment did not alter the basal Ca^{2+} levels. Application of cBIMPs resulted in enhanced Ca^{2+} signals in response to low [CCh] (Fig. 7*A*). The enhancing effects of cBIMPs were only evident in cells that responded minimally to CCh, indicating that PKA sensitizes $InsP_3R2$ to low levels of stimulation. This effect was manifested as either a potentiation of a minimal response or alternatively generation of a response following cBIMPs incubation, which was not previously evident in the absence of PKA activation (see examples in Fig. 7*A*). Following washout of cBIMPs, the response was again reduced to pre-PKA activation levels. Cells stably expressing $InsP_3R2$-S937A and transiently expressing M3 receptors did not significantly differ in their concentration *versus* response relationship to CCh (EC_{50} 1.11 ± 0.023 *versus* 0.89 ± 0.02 μM; wild type- *versus* S937A-expressing cells). These data indicate that mutation of S937A *per se* did not adversely influence the activity of $InsP_3R$. However, in contrast to the $InsP_3R2$ wild type cells, treatment of cells stably expressing $InsP_3R2$-S937A with cBIMPs failed in nine experimental runs from three separate transfections totaling 595 cells representative of various response patterns to result in enhanced CCh-induced Ca^{2+} signals (Fig. 7*B*). These results indicate that the sole effect of cBIMPs on $InsP_3R2$ is to induce the phosphorylation of Ser^{937}.

DISCUSSION

Cross-talk between the cAMP- and Ca^{2+}-signaling pathways can allow efficient regulation of the temporal and spatial aspects of cellular Ca^{2+} signals. This shaping of Ca^{2+} signals is thought to account for the wide range of physiological effects of intracellular Ca^{2+}. Understanding the molecular determinants behind this cross-talk is important in gaining a clearer picture of cell function and may provide targets for possible pharmaceutical interventions. Phosphorylation of $InsP_3R$ by PKA constitutes a means of regulating Ca^{2+} signaling by directly altering the Ca^{2+} release event. We have described an $InsP_3R2$-specific and receptor-distinct mechanism that may account for enhanced Ca^{2+} signaling in response to cAMP in cells expressing

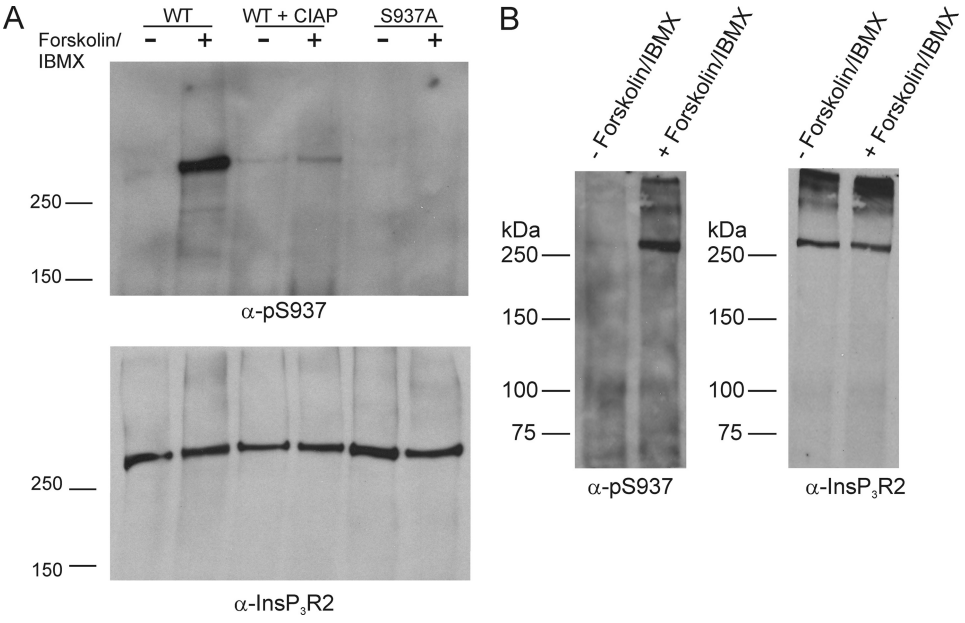

FIGURE 6. **PKA phosphorylates full-length mouse $InsP_3R2$ at Ser^{937}.** Wild type and S937A mutated full-length mouse $InsP_3R2$ were expressed in COS-7 cells. The cells were treated with forskolin and IBMX, and $InsP_3R2$ proteins were immunoprecipitated and separated by PAGE. *A*, results of a Western blot probed with α-$Ser(P)^{937}$. The antibody recognized a band at the appropriate size in the wild type sample but not in a parallel sample treated with calf intestine alkaline phosphatase prior to PAGE. The antibody also failed to recognize a band in the S937A mutant sample. The *lower panel* shows a Western blot on the same membrane after stripping and reprobing with an α-$InsP_3R2$ antibody, indicating equal expression in all samples. *B*, parotid acinar cells were isolated from mice and left untreated or treated with forskolin + IBMX. $InsP_3R2$ was immunoprecipitated from the samples and separated by PAGE. The *left panel* shows a Western blot of samples probed with α-$Ser(P)^{937}$. The antibody recognizes an appropriate band in the forskolin/IBMX-treated sample. The *right panel* shows a Western blot from the same membrane after stripping and reprobing with an antibody against $InsP_3R2$.

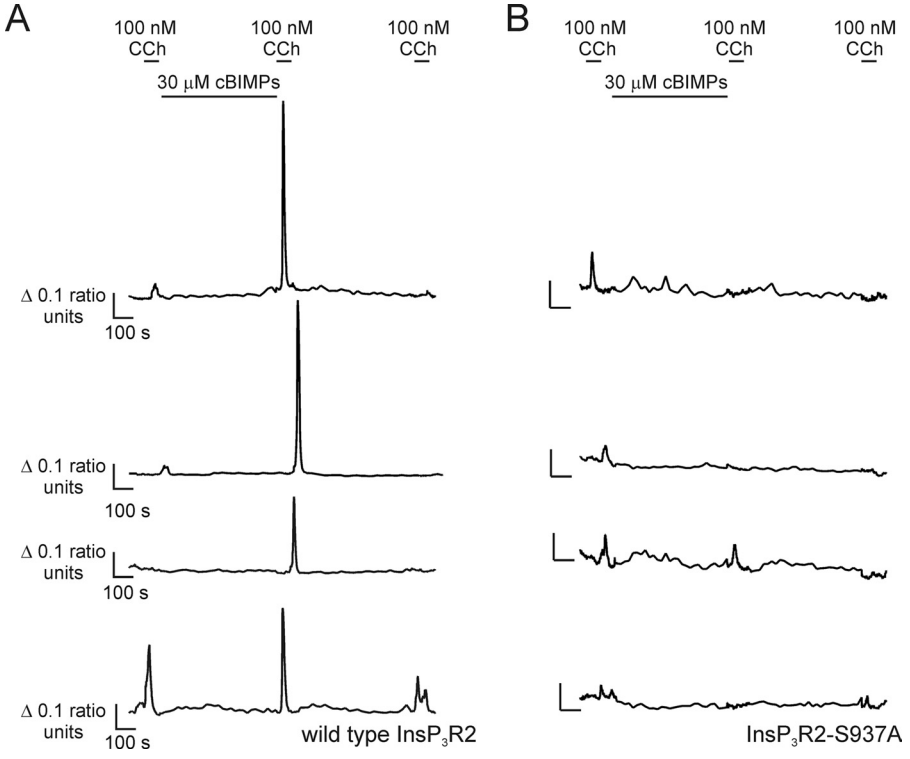

FIGURE 7. **cBIMPs enhances muscarinic receptor-induced Ca^{2+} transients in cells stably expressing wild type, but not S937A mutated $InsP_3R2$.** Stable DT40 cell lines were generated expressing wild type (DT40-InsP3R2) or S937A mutated (DT40-$InsP_3R2$-S937A) $InsP_3R2$. Cells were transfected with cDNA expressing M3R, and Fura-2 measurements were made on cells treated with CCh in the presence or absence of cBIMPs, as indicated. In these experiments, the acquisition rate was decreased between CCh stimulations. *A*, examples of the effects of cBIMPs on DT40-$InsP_3R2$ cells from four independent experiments; *B*, examples of responses in four independent experiments with DT40-$InsP_3R2$-S937A cells.

$InsP_3R2$. Specifically, PKA phosphorylation of a unique serine residue (Ser^{937}) increases the single channel P_o and Ca^{2+} release activity of $InsP_3R2$.

Phosphorylation of Ser^{937} in $InsP_3R2$ clearly leads to enhanced channel activity, but the ultimate molecular mechanism behind this effect is still a major unanswered question. We have recently identified effects of phosphorylation on $InsP_3R1$ channel activity by examining changes in single channel properties in phosphomimetic mutations of this isoform (20). Specifically, phosphorylation is thought to increase channel activity primarily by altering the probability of the channel exhibiting a high P_o "burst" phase. It is currently unknown whether PKA phosphorylation of $InsP_3R2$ exerts similar effects on this isoform. Analysis of an S937E/D phosphomimetic mutation could yield further mechanistic insights about the enhancing effects of PKA on $InsP_3R2$.

In addition to remaining mechanistic questions, an understanding of the physiological consequence of $InsP_3R2$ phosphorylation is lacking. Questions regarding the physiological significance of $InsP_3R$ phosphorylation will be greatly aided by the analysis of $InsP_3R2$ knock-out mice (10, 11, 51). Cardiac myocytes, liver hepatocytes, and astrocytes all express $InsP_3R2$ predominantly (8, 9). Analysis of agonist-induced Ca^{2+} signaling in astrocytes showed that acetylcholine, glutamate, and bradykinin-induced Ca^{2+} signals were completely absent in cells from $InsP_3R2$-KO mice (10). As such, modulation of $InsP_3R2$ by PKA and other mechanism would probably be important for astrocytic Ca^{2+} signaling. Similarly, activation of endothelin receptors in atrial myocytes produces arrhythmogenic Ca^{2+} signals that are eliminated in cells from $InsP_3R2$-KO mice (11). β-Adrenergic activation is known to modulate a range of proteins involved in cardiac Ca^{2+} handling (52). Enhanced $InsP_3R2$ Ca^{2+} sig-

naling by this pathway may exacerbate the arrhythmogenic potential of endothelin receptor activation. Finally, cAMP production is known to potentiate $InsP_3$-induced Ca^{2+} signaling in hepatocytes, where $InsP_3R2$ is the predominant isoform (13, 27). Phosphorylation of Ser^{937} of $InsP_3R2$ in hepatocytes could mediate this effect. Consistent with this idea, Ser^{937} was identified by mass spectroscopy as being phosphorylated in a global screen of hepatic phosphoproteins (53). The role of PKA phosphorylation of $InsP_3R2$ in tissues such as liver and heart should be the subject of further study.

The effects of PKA phosphorylation on $InsP_3R2$ were only evident at low levels of stimulation. $InsP_3R2$ localization is correlated with sites of Ca^{2+} wave initiation in hepatocytes (54, 55). Similarly, regions of astrocyte ER that exhibit enhanced Ca^{2+} release are enriched with $InsP_3R2$ (56). These results indicate that $InsP_3R2$ might be involved with initiating and propagating Ca^{2+} waves in these cells. Sensitizing $InsP_3R2$ to lower levels of $InsP_3$ by PKA phosphorylation could lower the threshold for initiating global Ca^{2+} transients. A hierarchy of Ca^{2+} signals is produced in response to $InsP_3$, ranging from Ca^{2+} puffs involving a few $InsP_3R$ to Ca^{2+} waves that recruit multiple Ca^{2+} release sites (57–59). Similarly, phosphorylation of a few $InsP_3R2$s in a cluster could increase the probability that an elementary Ca^{2+} signal will result in a global Ca^{2+} wave.

In summary, the results presented here add significantly to our knowledge of the functional effects and the molecular determinants of PKA regulation of $InsP_3R2$. The physiological importance of $InsP_3R2$ is only beginning to be understood. It should be noted, however, that this isoform is expressed to some extent in most mammalian cells (8). This suggests that enhancing $InsP_3R2$ activity by PKA will have profound effects on Ca^{2+} signaling and cell function in many different physiological contexts. Similarly, phosphorylation of $InsP_3R2$ by other kinases, including PKC (60), Ca^{2+} calmodulin-dependent protein kinase II (61), and Src kinase (62), has been reported. These and other kinases are thought to impact Ca^{2+} signaling by regulating $InsP_3R2$ activity, but knowledge of phosphorylation sites is lacking. Application of the fragment-based approach described here should help to identify the molecular determinants behind the effects of kinases other than PKA.

Acknowledgment—We thank Lyndee Knowlton for excellent technical assistance.

REFERENCES

1. Berridge, M. J. (1993) *Nature* **361,** 315–325
2. Bruce, J. I., Straub, S. V., and Yule, D. I. (2003) *Cell Calcium* **34,** 431–444
3. Natarajan, M., Lin, K. M., Hsueh, R. C., Sternweis, P. C., and Ranganathan, R. (2006) *Nat. Cell Biol.* **8,** 571–580
4. Bruce, J. I., Shuttleworth, T. J., Giovannucci, D. R., and Yule, D. I. (2002) *J. Biol. Chem.* **277,** 1340–1348
5. Straub, S. V., Wagner, L. E., 2nd, Bruce, J. I., and Yule, D. I. (2004) *Biol. Res.* **37,** 593–602
6. Kang, G., Joseph, J. W., Chepurny, O. G., Monaco, M., Wheeler, M. B., Bos, J. L., Schwede, F., Genieser, H. G., and Holz, G. G. (2003) *J. Biol. Chem.* **278,** 8279–8285
7. Taylor, C. W., Genazzani, A. A., and Morris, S. A. (1999) *Cell Calcium* **26,** 237–251
8. Wojcikiewicz, R. J. (1995) *J. Biol. Chem.* **270,** 11678–11683
9. Holtzclaw, L. A., Pandhit, S., Bare, D. J., Mignery, G. A., and Russell, J. T. (2002) *Glia* **39,** 69–84
10. Petravicz, J., Fiacco, T. A., and McCarthy, K. D. (2008) *J. Neurosci.* **28,** 4967–4973
11. Li, X., Zima, A. V., Sheikh, F., Blatter, L. A., and Chen, J. (2005) *Circ. Res.* **96,** 1274–1281
12. Zhang, X., Wen, J., Bidasee, K. R., Besch, H. R., Jr., Wojcikiewicz, R. J., Lee, B., and Rubin, R. P. (1999) *Biochem. J.* **340,** 519–527
13. Burgess, G. M., Bird, G. S., Obie, J. F., and Putney, J. W., Jr. (1991) *J. Biol. Chem.* **266,** 4772–4781
14. Hirono, C., Sugita, M., Furuya, K., Yamagishi, S., and Shiba, Y. (1998) *J. Membr. Biol.* **164,** 197–203
15. Walaas, S. I., Nairn, A. C., and Greengard, P. (1986) *J. Neurosci.* **6,** 954–961
16. Supattapone, S., Danoff, S. K., Theibert, A., Joseph, S. K., Steiner, J., and Snyder, S. H. (1988) *Proc. Natl. Acad. Sci. U.S.A.* **85,** 8747–8750
17. Volpe, P., and Alderson-Lang, B. H. (1990) *Am. J. Physiol.* **258,** C1086–C1091
18. Wagner, L. E., 2nd, Li, W. H., and Yule, D. I. (2003) *J. Biol. Chem.* **278,** 45811–45817
19. Wagner, L. E., 2nd, Li, W. H., Joseph, S. K., and Yule, D. I. (2004) *J. Biol. Chem.* **279,** 46242–46252
20. Wagner, L. E., 2nd, Joseph, S. K., and Yule, D. I. (2008) *J. Physiol.* **586,** 3577–3596
21. Wojcikiewicz, R. J., and Luo, S. G. (1998) *J. Biol. Chem.* **273,** 5670–5677
22. Soulsby, M. D., and Wojcikiewicz, R. J. (2005) *Biochem. J.* **392,** 493–497
23. Melvin, J. E., Yule, D., Shuttleworth, T., and Begenisich, T. (2005) *Annu. Rev. Physiol.* **67,** 445–469
24. Giovannucci, D. R., Groblewski, G. E., Sneyd, J., and Yule, D. I. (2000) *J. Biol. Chem.* **275,** 33704–33711
25. Straub, S. V., Giovannucci, D. R., Bruce, J. I., and Yule, D. I. (2002) *J. Biol. Chem.* **277,** 31949–31956
26. Regimbald-Dumas, Y., Arguin, G., Fregeau, M. O., and Guillemette, G. (2007) *J. Cell. Biochem.* **101,** 609–618
27. Hajnóczky, G., Gao, E., Nomura, T., Hoek, J. B., and Thomas, A. P. (1993) *Biochem. J.* **293,** 413–422
28. Soulsby, M. D., and Wojcikiewicz, R. J. (2007) *Cell Calcium* **42,** 261–270
29. Iwai, M., Tateishi, Y., Hattori, M., Mizutani, A., Nakamura, T., Futatsugi, A., Inoue, T., Furuichi, T., Michikawa, T., and Mikoshiba, K. (2005) *J. Biol. Chem.* **280,** 10305–10317
30. Wang, W., and Malcolm, B. A. (2002) *Methods Mol. Biol.* **182,** 37–43
31. Betzenhauser, M. J., Wagner, L. E., 2nd, Iwai, M., Michikawa, T., Mikoshiba, K., and Yule, D. I. (2008) *J. Biol. Chem.* **283,** 21579–21587
32. Betzenhauser, M. J., Wagner, L. E., 2nd, Won, J. H., and Yule, D. I. (2008) *Methods* **46,** 177–182
33. Wagner, L. E., 2nd, Betzenhauser, M. J., and Yule, D. I. (2006) *J. Biol. Chem.* **281,** 17410–17419
34. Dellis, O., Dedos, S. G., Tovey, S. C., Taufiq-Ur-Rahman, Dubel, S. J., and Taylor, C. W. (2006) *Science* **313,** 229–233
35. Dellis, O., Rossi, A. M., Dedos, S. G., and Taylor, C. W. (2008) *J. Biol. Chem.* **283,** 751–755
36. Wojcikiewicz, R. J., and He, Y. (1995) *Biochem. Biophys. Res. Commun.* **213,** 334–341
37. Swatton, J. E., and Taylor, C. W. (2002) *J. Biol. Chem.* **277,** 17571–17579
38. Joseph, S. K., Lin, C., Pierson, S., Thomas, A. P., and Maranto, A. R. (1995) *J. Biol. Chem.* **270,** 23310–23316
39. Maes, K., Missiaen, L., De Smet, P., Vanlingen, S., Callewaert, G., Parys, J. B., and De Smedt, H. (2000) *Cell Calcium* **27,** 257–267
40. Sugawara, H., Kurosaki, M., Takata, M., and Kurosaki, T. (1997) *EMBO J.* **16,** 3078–3088
41. Schug, Z. T., da Fonseca, P. C., Bhanumathy, C. D., Wagner, L., 2nd, Zhang, X., Bailey, B., Morris, E. P., Yule, D. I., and Joseph, S. K. (2008) *J. Biol. Chem.* **283,** 2939–2948
42. Tovey, S. C., Dedos, S. G., Taylor, E. J., Church, J. E., and Taylor, C. W. (2008) *J. Cell Biol.* **183,** 297–311
43. Joseph, S. K., Bokkala, S., Boehning, D., and Zeigler, S. (2000) *J. Biol. Chem.* **275,** 16084–16090
44. Shabb, J. B. (2001) *Chem. Rev.* **101,** 2381–2411
45. Yoshikawa, F., Iwasaki, H., Michikawa, T., Furuichi, T., and Mikoshiba, K.

(1999) *J. Biol. Chem.* **274,** 316–327
46. Maes, K., Missiaen, L., Parys, J. B., De Smet, P., Sienaert, I., Waelkens, E., Callewaert, G., and De Smedt, H. (2001) *J. Biol. Chem.* **276,** 3492–3497
47. Khan, M. T., Wagner, L., 2nd, Yule, D. I., Bhanumathy, C., and Joseph, S. K. (2006) *J. Biol. Chem.* **281,** 3731–3737
48. Szado, T., Vanderheyden, V., Parys, J. B., De Smedt, H., Rietdorf, K., Kotelevets, L., Chastre, E., Khan, F., Landegren, U., Söderberg, O., Bootman, M. D., and Roderick, H. L. (2008) *Proc. Natl. Acad. Sci. U.S.A.* **105,** 2427–2432
49. Soulsby, M. D., Alzayady, K., Xu, Q., and Wojcikiewicz, R. J. (2004) *FEBS Lett.* **557,** 181–184
50. Pieper, A. A., Brat, D. J., O'Hearn, E., Krug, D. K., Kaplin, A. I., Takahashi, K., Greenberg, J. H., Ginty, D., Molliver, M. E., and Snyder, S. H. (2001) *Neuroscience* **102,** 433–444
51. Futatsugi, A., Nakamura, T., Yamada, M. K., Ebisui, E., Nakamura, K., Uchida, K., Kitaguchi, T., Takahashi-Iwanaga, H., Noda, T., Aruga, J., and Mikoshiba, K. (2005) *Science* **309,** 2232–2234
52. Bers, D. M. (2002) *Nature* **415,** 198–205
53. Villén, J., Beausoleil, S. A., Gerber, S. A., and Gygi, S. P. (2007) *Proc. Natl. Acad. Sci. U.S.A.* **104,** 1488–1493
54. Hirata, K., Pusl, T., O'Neill, A. F., Dranoff, J. A., and Nathanson, M. H. (2002) *Gastroenterology* **122,** 1088–1100
55. Hernandez, E., Leite, M. F., Guerra, M. T., Kruglov, E. A., Bruna-Romero, O., Rodrigues, M. A., Gomes, D. A., Giordano, F. J., Dranoff, J. A., and Nathanson, M. H. (2007) *J. Biol. Chem.* **282,** 10057–10067
56. Sheppard, C. A., Simpson, P. B., Sharp, A. H., Nucifora, F. C., Ross, C. A., Lange, G. D., and Russell, J. T. (1997) *J. Neurochem.* **68,** 2317–2327
57. Bootman, M. D., Berridge, M. J., and Lipp, P. (1997) *Cell* **91,** 367–373
58. Parker, I., Choi, J., and Yao, Y. (1996) *Cell Calcium* **20,** 105–121
59. Marchant, J. S., and Parker, I. (2001) *EMBO J.* **20,** 65–76
60. Arguin, G., Regimbald-Dumas, Y., Fregeau, M. O., Caron, A. Z., and Guillemette, G. (2007) *J. Endocrinol.* **192,** 659–668
61. Bare, D. J., Kettlun, C. S., Liang, M., Bers, D. M., and Mignery, G. A. (2005) *J. Biol. Chem.* **280,** 15912–15920
62. Yuan, Z., Cai, T., Tian, J., Ivanov, A. V., Giovannucci, D. R., and Xie, Z. (2005) *Mol. Biol. Cell* **16,** 4034–4045